Science of the Total Environment 721 (2020) 137664

Contents lists available at ScienceDirect

Science of the Total Environment

journal homepage: www.elsevier.com/locate/scitotenv

Heat wave trends in Southeast Asia during 1979–2018: The impact of humidity

Xian-Xiang Li *

School of Atmospheric Sciences, Sun Yat-sen University, China
Southern Marine Science and Engineering Guangdong Laboratory (Zhuhai), China
Guangdong Province Key Laboratory for Climate Change and Natural Disaster Studies, Sun Yat-sen University, China

HIGHLIGHTS

- Heat waves are becoming more frequent, longer-lasting and more intense in most Southeast Asia.
- HWs based on minimum temperatures increase at higher rate than based on maximum temperatures.
- Wet-bulb temperature based HWs show larger increasing trends in Malay and Indochina Peninsulas.
- Nearly all HW metrics are significantly correlated with El Nino index, but IOD only impacts Java.
- Comparison with different reanalysis datasets demonstrates robustness of our findings.

GRAPHICAL ABSTRACT

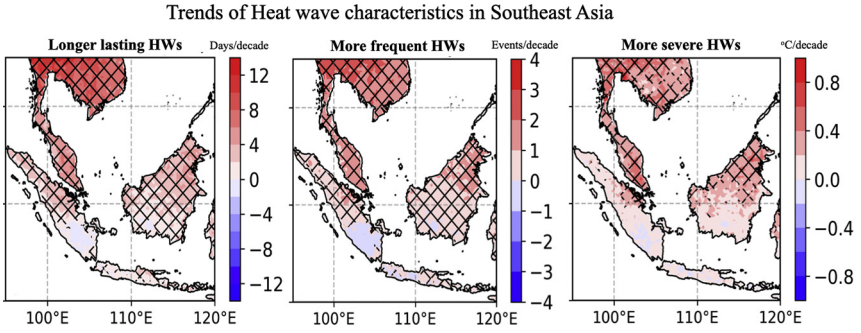

ARTICLE INFO

Article history:
Received 13 November 2019
Received in revised form 29 February 2020
Accepted 29 February 2020
Available online 5 March 2020

Editor: Scott Sheridan

Keywords:
Climate extreme
Heat stress
Wet-bulb temperature
Reanalysis
ERA5

ABSTRACT

In tropics, especially Southeast Asia (SEA), heat wave (HW) research is seriously scarce although several global studies have projected this region to be greatly susceptible to increasing HW events under climate change scenarios. Using the recently released ERA5 reanalysis data, we find that in most parts of SEA, HWs are becoming more frequent, longer-lasting and stronger, no matter using dry-bulb or wet-bulb temperatures to define HW. The increasing trends of HW characteristics based on minimum temperatures are larger than those based on maximum temperatures, suggesting an alarming situation of anomalously warm night. HW characteristics based on wet-bulb temperatures show higher increasing rates in the IndoChina Peninsula and Malay Peninsula than those based on dry-bulb temperatures. Nearly all HW characteristics are significantly correlated with El Niño index, but Indian Ocean Dipole only significantly impacts HW characteristics based on wet-bulb temperature in Java. Results derived from other reanalysis products exhibit general agreement with those from ERA5, lending support to the findings reported herein. This study highlights the different role of humidity in changing HW trends in different regions of SEA, and calls for attention to the associated risk of increasing nighttime temperatures during HWs.

* School of Atmospheric Sciences, Sun Yat-sen University, Zhuhai, Guangdong, China.
E-mail address: lixx98@mail.sysu.edu.cn.

https://doi.org/10.1016/j.scitotenv.2020.137664
0048-9697/

1. Introduction

A heat wave (HW) is usually defined broadly as prolonged period (usually several consecutive days) with temperature exceeding prescribed thresholds. Its specific definition, however, varies greatly among sectors and depends heavily on the purpose of the applications (Gosling et al., 2009). HWs can produce local and regional impacts on environment and society, including health (Mora et al., 2017; Xu et al., 2016), infrastructure (e.g., Li, 2018), and economy (Xia et al., 2018). For health, it is the sustained nature of heatwaves that impose more devastating impacts than extreme temperatures on a single day, since excessive human morbidity and mortality rates are generally associated with extreme temperatures in an extended period (Perkins-Kirkpatrick and Gibson, 2017). HW has been the most deadly natural hazard in Australia (Coates et al., 2014) and caused more deaths in US cities than all other weather events combined (NWS, 2018). Huang et al. (2018) also demonstrated the acute and cumulative effect of HW on mortality in Thailand, one of Southeast Asian countries characterized by hot and humid climate.

Humidity is another variable often involved in HW or heat stress definition (Sherwood, 2018), because high humidity may aggravate impacts of HWs on human thermoregualtion (Schär, 2016) and impair labor productivity (Dunne et al., 2013). In hot environment, evaporation is the primary means by which bodies cool. When temperature and humidity are high, evaporative cooling is restricted and the body core temperature may rise. But a normal human body's temperature is maintained within a very narrow limit of ± 1°C (Epstein and Moran, 2006), the body cannot adjust temperature if body temperature exceeds levels of certain threshold, which can cause detriments to physical and cognitive functions. Recent studies have found the combined temperature and humidity responsible for the high mortality in India and Pakistan during the 2015 HW (Wehner et al., 2016).

As the combined effect of temperature and humidity, the wet bulb temperature T_w is argued to be one of the best quantities in human health applications associated with heat stress in hot, humid environment (Davis et al., 2016). T_w is defined as the temperature achieved by an air parcel if we evaporate water into it until saturation at constant pressure. Increasing T_w reduces the human body's cooling ability. T_w establishes a clear thermodynamic limit on heat transfer that cannot be overcome by acclimatization or adaptation (Sherwood and Huber, 2010; Coffel et al., 2017). Sherwood and Huber (2010) proposed a concept of human survivability threshold based on T_w, with an upper limit at 35 °C; when T_w exceeds this upper limit, metabolic heat can no longer be dissipated. Although current observation of T_w rarely exceeded 31 °C (Sherwood and Huber, 2010), a recent HW event around the Persian Gulf saw a record T_w of 34.6 °C (Schär, 2016), very close to the critical threshold of 35 °C. Raymond et al. (2017) examined T_w extremes in US and found that humidity variations are more important than those of temperature in creating extreme T_w.

There are several other indices used in the literature to quantify the effect of humidity on heat stress, including apparent temperature (e.g., Li et al., 2018), wet-bulb global temperature (WBGT) (e.g., Willett and Sherwood, 2012), heat index (e.g., Russo et al., 2017), and equivalent temperature (Pielke Sr et al., 2004; Schoof et al., 2017). Unlike T_w which has a clearly established thermodynamic limit, most of these indices are significantly affected by local environmental, physiological, and sociological factors. Therefore, T_w is arguably more

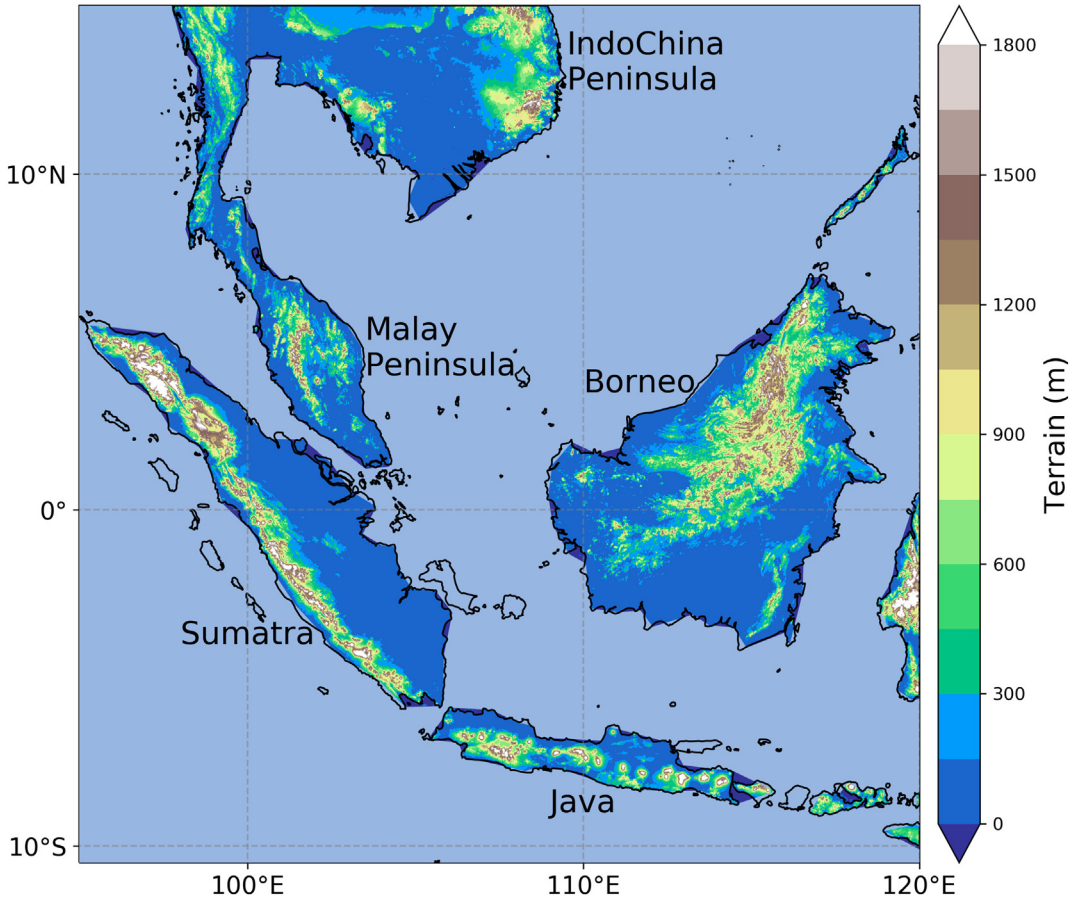

Fig. 1. Terrain of the study area, with the names of different regions.

suitable for long-term climate study of extreme heat events considering the impact of humidity.

In many parts of the world where long-term surface observations are limited or of poor quality, such as Southeast Asia (SEA), atmospheric reanalyses have provided a significant source of data for weather and climate research (Grotjahn et al., 2016). Reanalysis data consist of an optimal blend of observations and model simulations to represent the best estimate of the atmospheric state, and provide physically and dynamically consistent dataset over the period being reanalyzed, which are enforced by the data assimilation process. Moreover, the estimation of temperature extremes near the ground is usually difficult, since extreme values in instrumental data are susceptible to noise and bad data values and require very careful data quality control. Reanalysis data can eliminate bad data values by using the forecast fields, and thus are increasingly utilized in extreme climate event study (e.g., Li et al., 2018, Luo and Lau, 2018). The use of reanalysis data also extends the study to locations that do not have observational data readily available (Li et al., 2018, Hassim and Timbal, 2019).

In SEA region, while some regional studies of climate extreme indices have been carried out covering some countries (Manton et al., 2001; Caesar et al., 2011; Cheong et al., 2018), there have been no systematic investigations of HWs, especially on the effect of high humidity. This situation is alarming since the capacity to adapt and manage the risks of extreme heat is often limited in the tropics (IPCC, 2007). Recent studies have projected that most of the tropical regions will spend much of the year above the highest historical T_w by 2060–2080 under Representative Concentration Pathways (RCP) 8.5 scenario (Coffel et al., 2017), and the extent of exposure to maximum T_w above 31 °C will reach 20% of the land area in SEA (Im et al., 2018). Other projections also show the most striking changes in the tropics, with over 30 extra heatwave days per season, and 4–6 days increase of the longest heat wave event in SEA per °C of global temperature rise (Perkins-Kirkpatrick and Gibson, 2017).

In this study, we try to narrow this gap of HW research in SEA and explore the trends of HWs based on both dry- and wet-bulb temperatures. We use the new reanalysis dataset ERA5 to derive the extreme temperature data for SEA. By examining the differences of HWs based on dry- and wet-bulb temperatures, we will highlight the regional impact of humidity.

2. Data and method

2.1. Data

For such a data-scarce region as SEA, there are no long-term high-quality daily observational data available. This region is usually underrepresented in previous global studies (e.g., Perkins et al., 2012). Though several regional studies of temperature extremes have been performed (e.g., Caesar et al., 2011, Cheong et al., 2018), those station data remain unavailable to the research community. A gridded dataset of observed daily maximum and minimum temperatures for SEA, SA–OBS (Van den Besselaar et al., 2017) is available, but no humidity information exists. SA-OBS is based on station data provided by meteorological services of SEA countries, within a project called the Southeast Asian Climate Assessment and Dataset (SACA&D; http://sacad.database.bmkg.go.id). To overcome these problems, the new ERA5 reanalysis data (Copernicus Climate Change Service, 2017) produced by European Center for Medium-Range Weather Forecasting (ECMWF) is used in this study. As the successor of ERA-Interim (Dee et al., 2011), ERA5 reanalysis is produced using the Integrated Forecast System (IFS) cycle 41r2 with 4-D-Var data assimilation, at a horizontal resolution of ~31 km (~0.25°) and temporal resolution of 1 h. In addition to the higher resolutions, ERA5 assimilates more observational data from stations and satellites than ERA-Interim, and improves upon ERA-Interim in various other aspects including the better representation of tropospheric processes, better precipitation over land in the deep tropics, better soil moisture, and more consistent sea surface temperatures and sea ice (Hennermann and Berrisford, 2018). ERA5 has been used in several studies, and shown significant improvements in various aspects (e.g., Albergel et al., 2018, Chen et al., 2020, Hoffmann et al., 2019). Compared with previous reanalysis datasets, ERA5 demonstrated greatly reduced bias in surface air temperature (Betts et al., 2019; Graham et al., 2019; Mahto and Mishra, 2019), specific humidity (Graham et al., 2019), precipitation (Mahto and Mishra, 2019; Tarek et al., 2019), and wind speed (Graham et al., 2019).

The study period covers 1979 to 2018, with a spatial range between 95–120°E and 10°S–15°N (Fig. 1). The region is characterized by complex terrains and coastlines, and there is no distinct seasonal variation in most of the region. The hourly wet-bulb temperature T_w is calculated based on Davies-Jones (2008) using 2-m air temperature T, 2-m dewpoint temperature and surface pressure from ERA5. The daily maximum and minimum T and T_w are then calculated from the hourly data. Some preliminary comparisons between the ERA5-derived daily maximum and minimum T and T_w and observations (Changi climatic station in Singapore and SA-OBS) are presented in Figs. 2–4. The comparison with observations at Changi station (103.9826°E, 1.3678°N) shows that ERA5 underestimates T_{max} and overestimates T_{min}; however, the

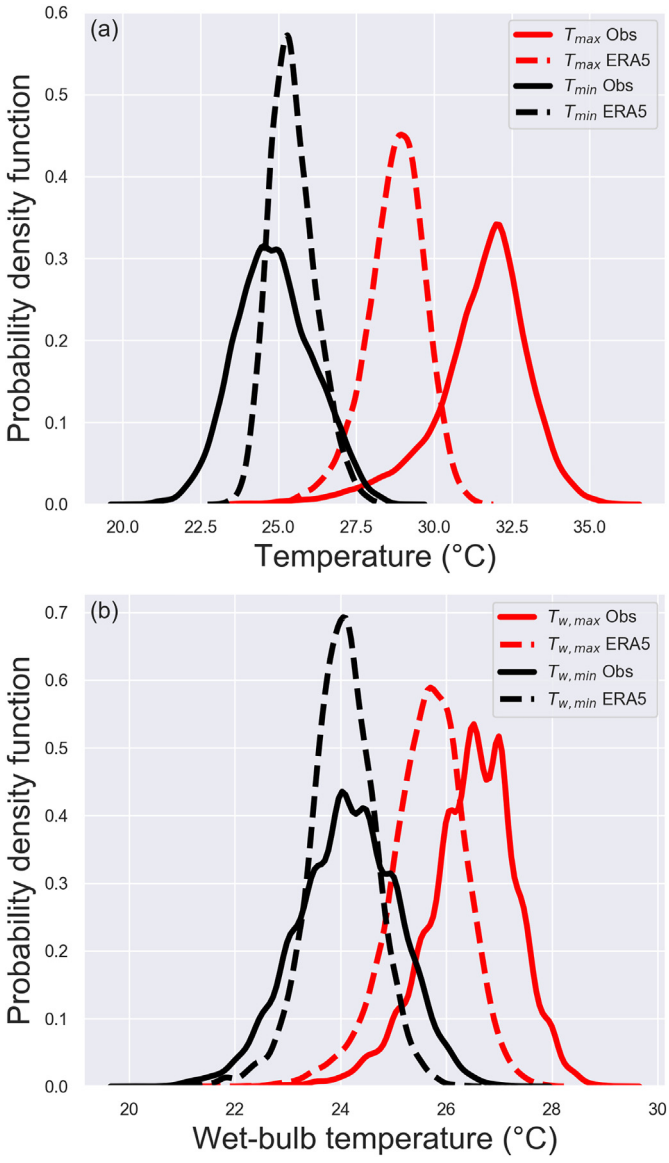

Fig. 2. Probability distribution of daily (a) T_{max} and T_{min}; (b) $T_{w,max}$ and $T_{w,min}$ from ERA5 and observations at Changi station in Singapore from 1982 to 2018.

variability of T_{max} is generally retained while the mean is shifted (Fig. 2a). For T_{min}, both the mean and variability are shifted towards the higher end (Fig. 2a). The situation of $T_{w,\ max}$ is similar to that of T_{max}, with less shit of mean (Fig. 2b). ERA5 produces good estimate of $T_{w,\ min}$ mean, with less extremes in the variability (Fig. 2b). Compared with SA-OBS, ERA5 also shows generally underestimated T_{max} (Fig. 3) and overestimated T_{min} (Fig. 4). Specifically, ERA5 produces higher T_{max} in eastern IndoChina Peninsula, northern Borneo and the middle of Malay Peninsula (Fig. 3). Relatively higher overestimation of T_{min} can be found in the IndoChina Peninsula, southern Borneo, and the west coast of Sumatra (Fig. 3). Most of these overestimations seem associated with high-altitude areas (see Fig. 1 for the terrain in SEA). One minor reason for these discrepancies is that we derive daily maximum and minimum temperatures based on hourly data, and hence miss the

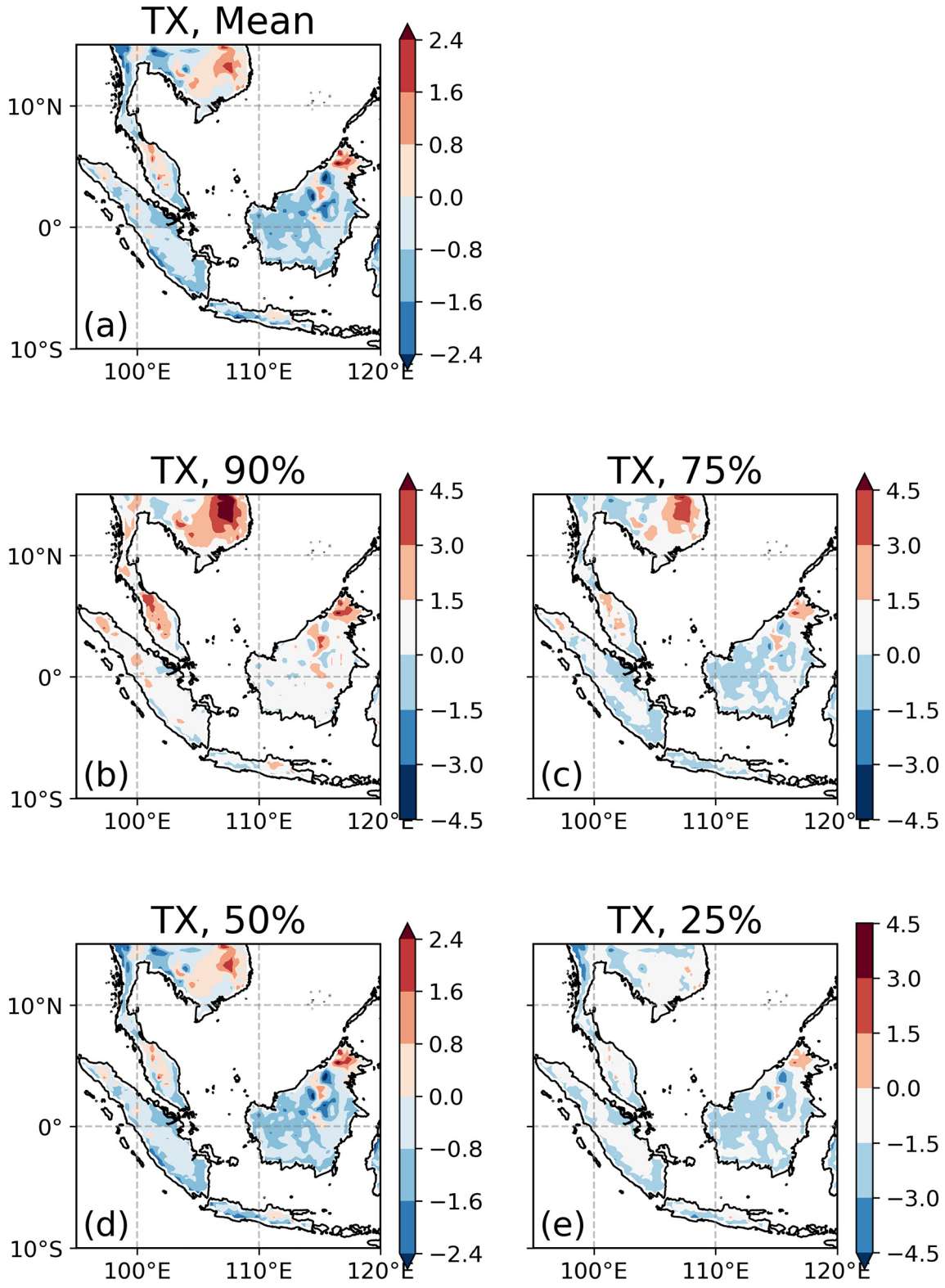

Fig. 3. The daily T_{max} bias (°C) of ERA5 compared with SA-OBS. (a) The mean of the bias; (b) 90%; (c) 75%; (d) 50%; and (e) 25% percentiles of the bias.

sub-hourly extreme temperatures. A further comparison with data derived from ERA5 sub-hourly data (not shown here) shows that the sub-hourly extreme temperatures can slightly improve the agreement of the daily minimum temperature, but have no effect in that of the daily maximum temperature. Here we still choose to use hourly data, so that daily dry- and wet-bulb temperatures are derived in the same way.

To test the robustness of the conclusions drawn from ERA5, several other reanalysis datasets are also used to derive HW trends in SEA, including ERA-Interim (Dee et al., 2011), the National Aeronautics and Space Administration (NASA) Modern-Era Retrospective Analysis for Research and Applications 2 (MERRA-2; Gelaro et al., 2017), and the National Centers for Environmental Prediction (NCEP) Climate Forecast System Reanalysis (CFSR; Saha et al., 2010). Unlike ERA5 or ERA-

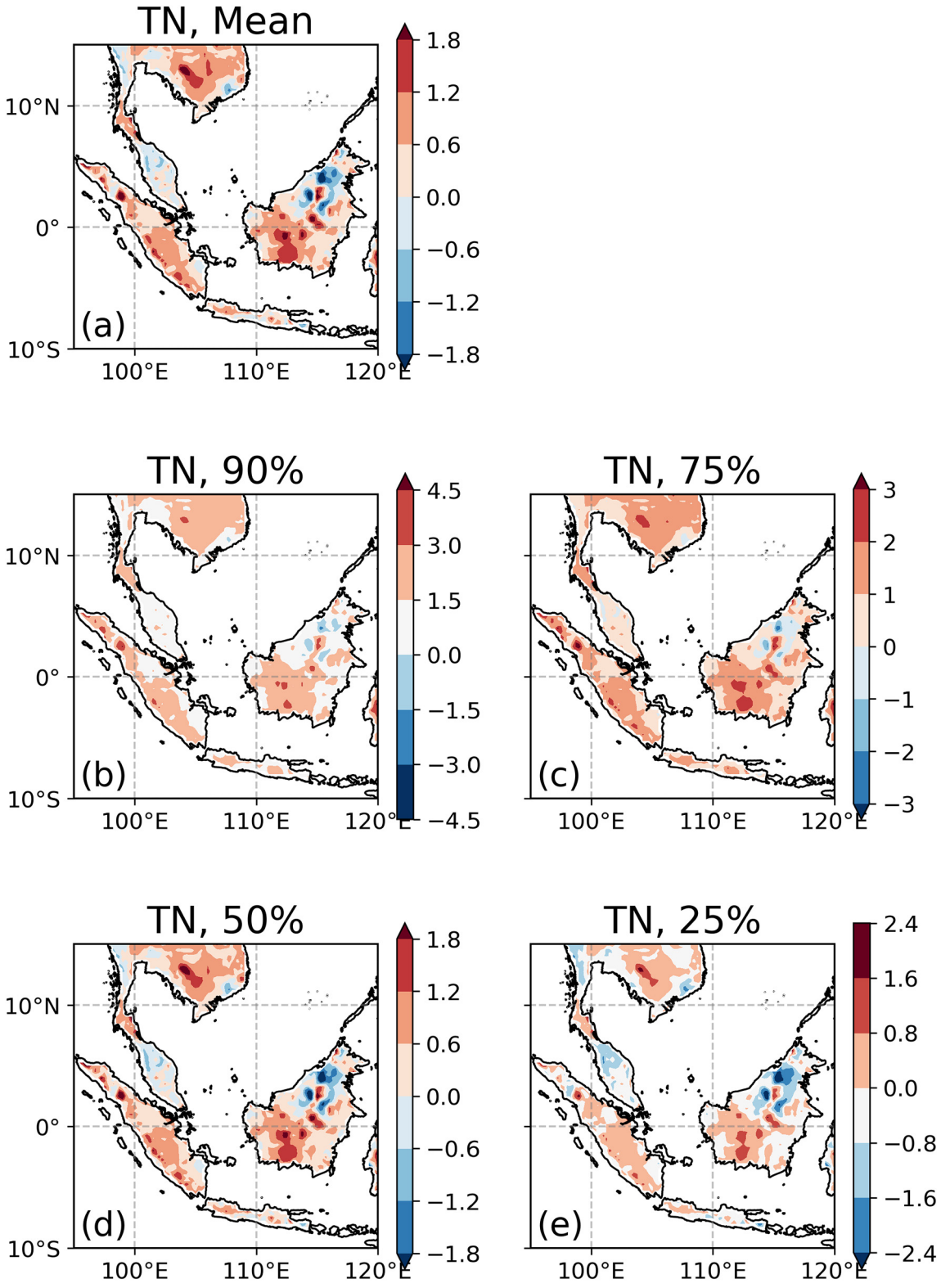

Fig. 4. The daily T_{min} bias (°C) of ERA5 compared with SA-OBS. (a) The mean of the bias; (b) 90%; (c) 75%; (d) 50%; and (e) 25% percentiles of the bias.

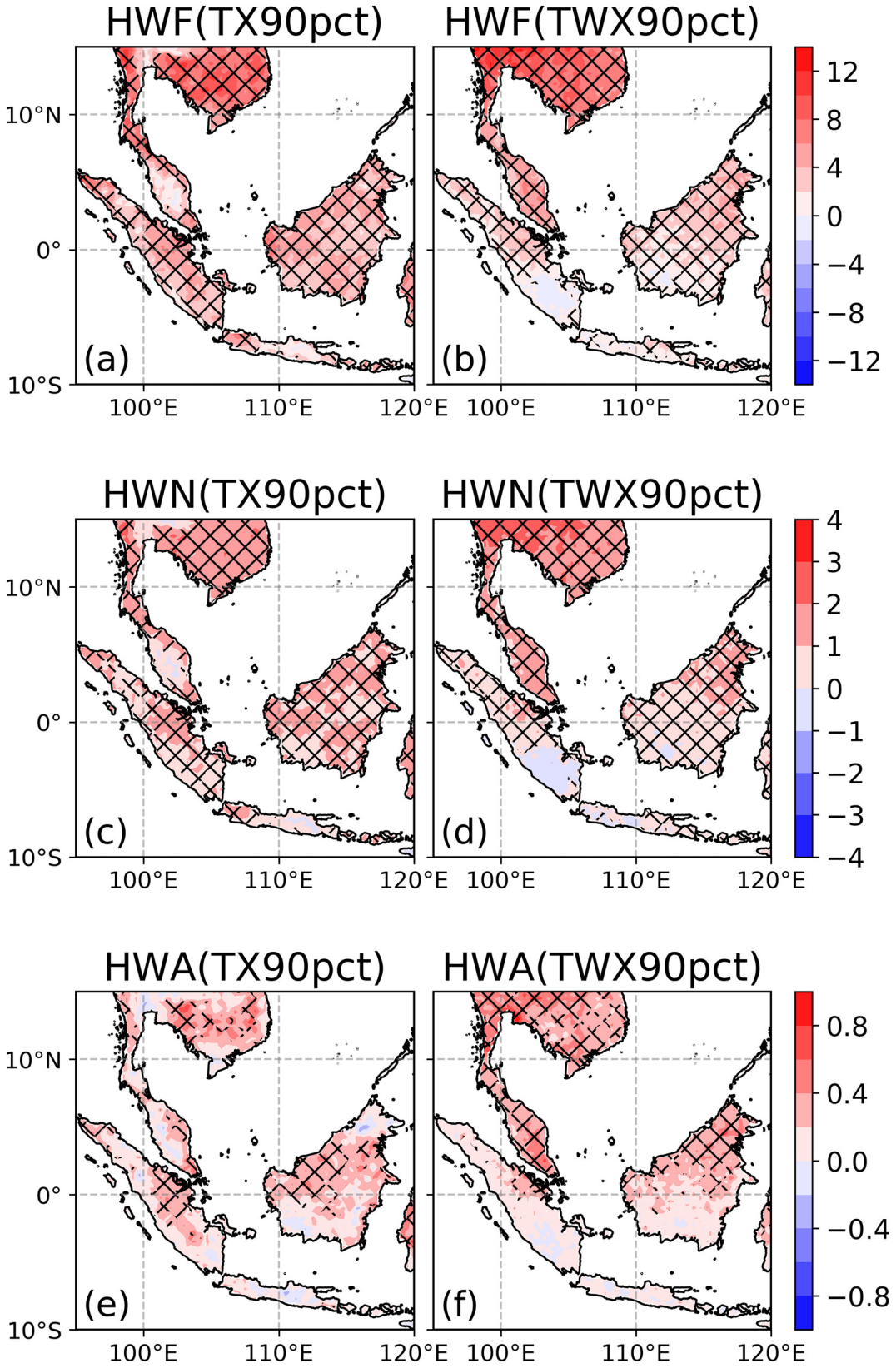

Fig. 5. Heat wave trends of (a,b) HWF (number of days participating in an event); (c,d) HWN (number of heat wave events); and (e,f) HWA (maximum intensity of the hottest event) based on (a,c,e) TX90pct and (b,d,f) TWX90pct. Trends are calculated for 1979–2018 using the non-parametric Theil-Sen slope estimator at 95% confidence level. The hatches represent areas with statistical significant trends. The units are days/decade for HWF, events/decade for HWN and °C/decade for HWA.

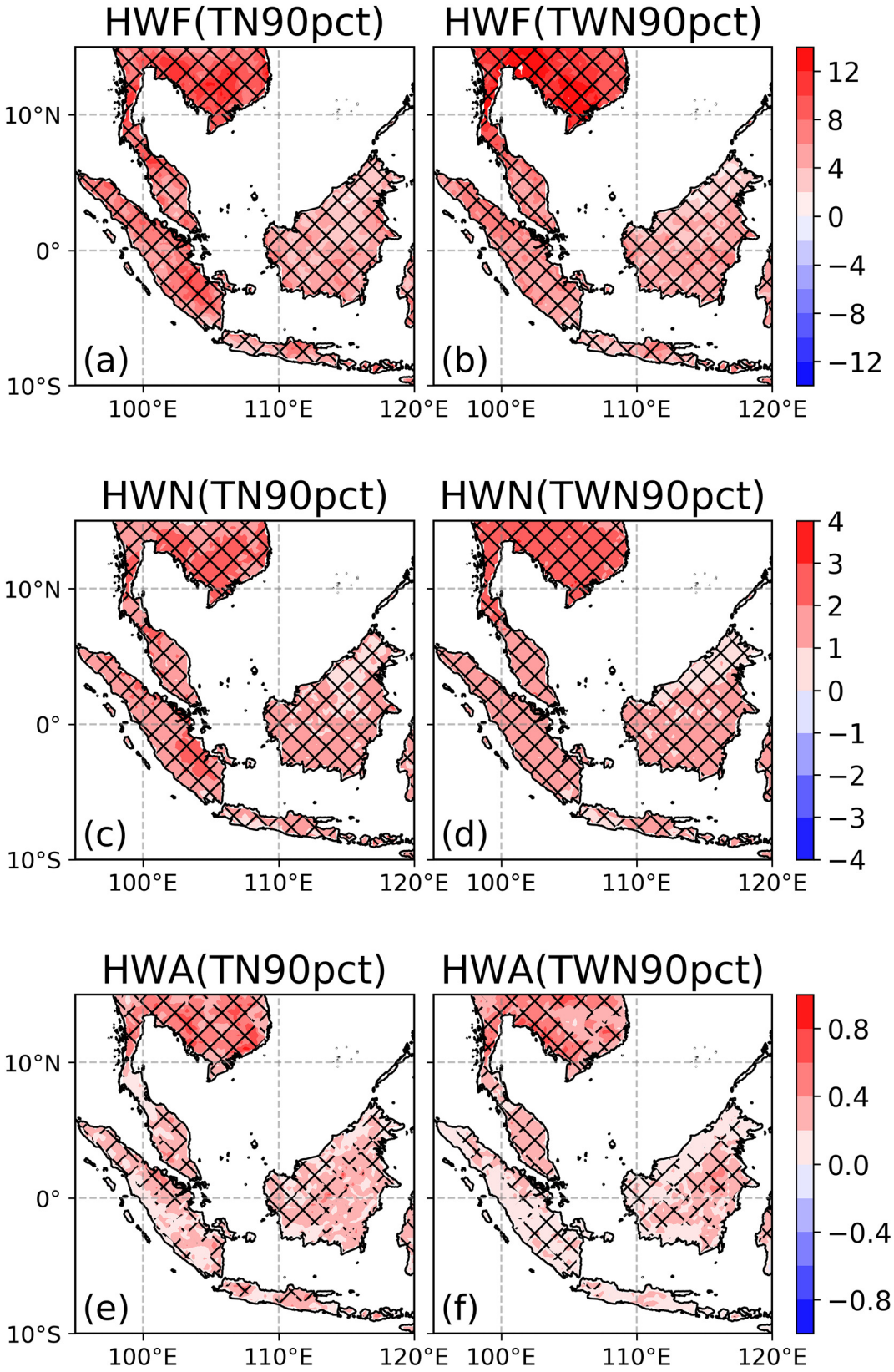

Fig. 6. Heat wave trends of (a,b) HWF (number of days participating in an event); (c,d) HWN (number of heat wave events); and (e,f) HWA (maximum intensity of the hottest event) based on (a,c,e) TN90pct and (b,d,f) TWN90pct. Trends are calculated for 1979–2018 using the non-parametric Theil-Sen slope estimator at 95% confidence level. The hatches represent areas with statistical significant trends. The units are days/decade for HWF, events/decade for HWN and °C/decade for HWA.

Interim, CFSR and MERRA-2 did not assimilate 2-m temperature and humidity.

The El Niño-Southern Oscillation (ENSO) and Indian Ocean Dipole (IOD) have great impact on SEA climate (e.g., Saji et al., 1999, D'Arrigo and Wilson, 2008, Tangang et al., 2008, Hong and Li, 2009, Villafuerte and Matsumoto, 2015, Tangang et al., 2017). In order to study the impacts of ENSO on HWs in SEA, we use the Oceanic Niño index (ONI) obtained from NOAA Climate Prediction Center (https://origin.cpc.ncep.noaa.gov/products/analysis_monitoring/ensostuff/ONI_v5.php) to quantify ENSO variability. ONI measures the sea surface temperature (SST) anomaly at 5°N - 5°S, 170°W - 120°W, and is calculated as a 3-month running mean. The ONI usually peaks during the boreal winter DJF (December, January and February), and ONI in DJF is used here. The IOD is commonly measured by the dipole mode index (DMI), which is calculated as the difference between SSTs in the western (50°E to 70°E and 10°S to 10°N) and eastern (90°E to 110°E and 10°S to 0°S) equatorial Indian Ocean. A positive (negative) IOD is associated with a cooling (warming) off the Sumatra coast and a warming (cooling) over the western equatorial Indian Ocean. The monthly DMI data was obtained from NOAA (https://www.cpc.ncep.noaa.gov/products/GODAS/multiora/index/mnth.ersstv5.clim19812010.dmi_current.txt) and the yearly mean DMI is used. The non-parametric Spearman's correlation is used to quantify the correlation between ONI and DMI and HW characteristics.

2.2. Heat wave definition

We use relative thresholds in HW definitions. Four thresholds are employed to calculate HWs over the entire year:

1. TX90pct (TN90pct): the threshold is the calendar-day 90th percentile based on a 15-day moving average for daily T_{max} (T_{min}).
2. TWX90pct (TWN90pct): the threshold is the calendar-day 90th percentile based on a 15-day moving average for daily $T_{w,\,max}$ ($T_{w,\,min}$).

In this way, the 90th percentile is relative to the time of year as well as the location. The HW is then defined when the respective threshold is exceeded for at least three consecutive days.

For each of the four HW definitions, various characteristics of HW frequency, duration and intensity are calculated for each year (Fischer and Schär, 2010; Perkins and Alexander, 2013):

1. HWF: the total number of days satisfying HW definition;
2. HWN: the total number of HW events; and

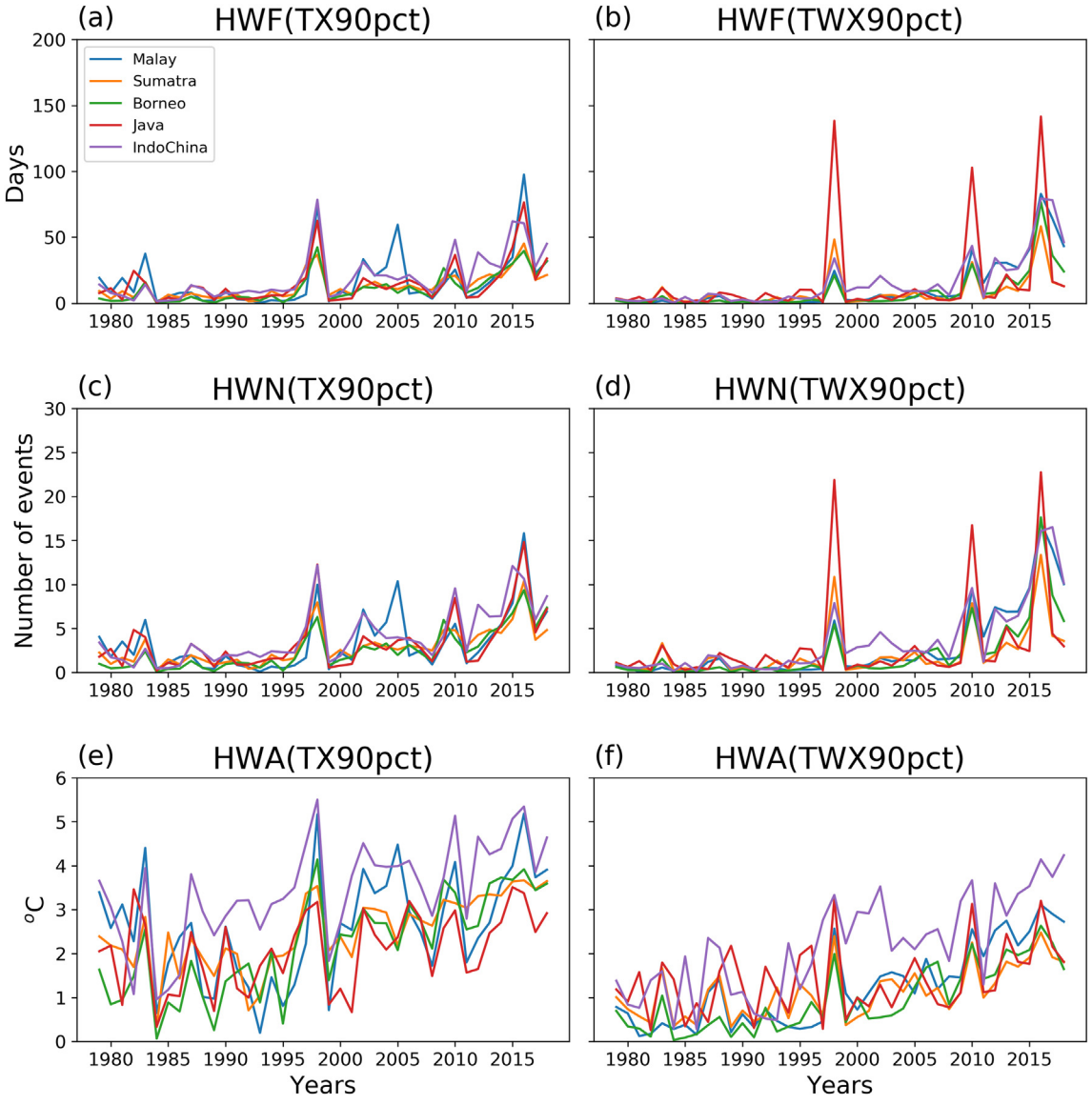

Fig. 7. Time series of (a,b) HWF; (c,d) HWN; and (e,f) HWA based on (a,c,e) TX90pct and (b,d,f) TWX90pct for the five regions in SEA.

3. HWA: the intensity of the hottest day (amplitude) of the hottest event. Please note this definition is the same as in Perkins and Alexander (2013), but different from those used in other studies, which used absolute temperature for HWA (Fischer and Schär, 2010; Perkins et al., 2012).

The trends of various HW characteristics in each grid are calculated using the non-parametric Theil-Sen slope estimator (Sen, 1968), and the statistical significance of these trends is tested using Mann-Kendall test (Mann, 1945) at the 95% level. Since extreme events like HWs by definition occur within the tail of a distribution, non-parametric methods are highly recommended and widely applied for the trend estimation of climate extremes.

3. Results

3.1. Heatwave trends

The HWF (the yearly total number of HW days) based on maximum T (Fig. 5a) and T_w (Fig. 5b) shows statistically significant increasing trends in IndoChina Peninsula and Borneo, and non-significant smaller increasing trends in Java. In Malay Peninsula, HWF based on T_{max} shows small, non-significant increasing trends along the west coast and the mountain ranges in the middle (Fig. 5a). In southern Sumatra, HWF based on $T_{w,\ max}$ exhibits a small decreasing trends, which are not statistically significant (Fig. 5b). Both HWF(TX90pct) and HWF (TWX90pct) have a general south-to-north gradient, from 1 day/decade in Java to about 10 days/decade in IndoChina Peninsula. The spatial patterns of HWN trends (Fig. 5c, d) highly resemble those of HWF. The trends for HWA (the maximum intensity of the yearly hottest event) based on maximum T (Fig. 5e) and maximum T_w (Fig. 5f) are less spatially coherent, and no statistically significant trends can be found in Java. Statistically significant trends of HWA(TX90pct) can be seen in parts of IndoChina Peninsula, the east coast of Malay Peninsula, and parts of Sumatra and Borneo. Compared with HWA(TX90pct), it seems that more areas are showing statistically significant trends of HWA(TWX90pct), in most part of the IndoChina Peninsula, the whole Malay Peninsula, northern Borneo and a small part of Sumatra.

The trends of HW characteristics based on minimum T and T_w are shown in Fig. 6. The prominent feature is that all trends are positive almost everywhere, indicating a general increasing trend of temperature extremes in SEA. HWF (Fig. 6a,b) increases by about 12 days/decade in the IndoChina Peninsula, and below 4 days/decade in most of other regions. HWF(TWN90pct) (Fig. 6b) is higher than HWF(TN90pct)

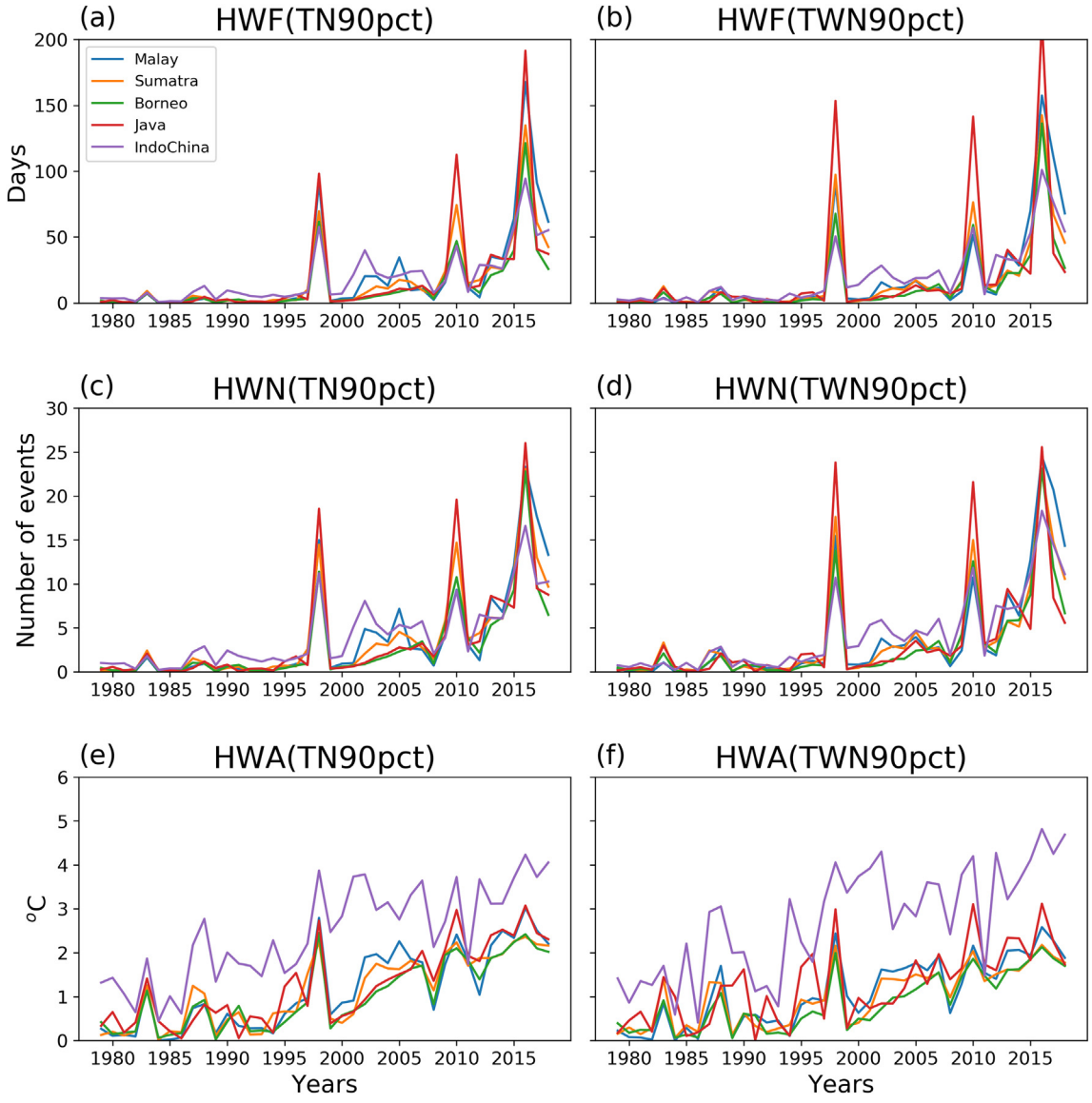

Fig. 8. Time series of (a,b) HWF; (c,d) HWN; and (e,f) HWA based on (a,c,e) TN90pct and (b,d,f) TWN90pct for the five regions in SEA.

(Fig. 6a) in the IndoChina Peninsula, while they are comparable in most of other regions. In Borneo, the HWF increasing trends based on the maximum temperatures (Fig. 5b) are higher in the north, while those based on the minimum temperatures are higher in the southern Borneo. As noted above, HWN trends (Fig. 6c,d) follow closely the spatial patterns of HWF. There are less areas showing statistically significant increasing trends of HWA(TWN90pct) (Fig. 6f) than HWA(TN90pct) (Fig. 6e), which is reverse to the case of HWA based on the maximum temperatures (Fig. 5e,f). In Java, HWA shows small and mostly non-significant increasing trends; however, these trends are still larger than their counterparts based on the maximum temperatures (Fig. 5e, f). Except in the IndoChina Peninsula, the trends of HWA are generally small, mostly around 0–0.4 °C/decade. This can be attributed to the narrow range of T and particularly T_w in SEA.

Comparing Figs. 5 and 6, it can be seen that the HW characteristics based on the minimum temperatures are more spatially coherent than those based on the maximum temperatures. Also the trends based on the minimum temperatures are larger than their counterparts based on the maximum temperatures. This is consistent with previous studies of temperature extremes in this region (e.g. Manton et al., 2001, Caesar et al., 2011, Cheong et al., 2018) or globally (e.g. Alexander et al., 2006), which demonstrated that minimum temperatures are increasing at a higher rate than maximum temperatures. While high daytime maximum temperature is known to affect human life and health, anomalously warm nighttime minimum temperatures have been linked to increased mortality and detrimental health effects in high-impact HWs across the globe during the past few decades (Nissan et al., 2017). Therefore, the higher increasing trends of temperature extremes based on minimum temperatures are alarming and call for more necessary mitigation and adaptation measures targeting at lowering nighttime temperatures.

Shown in Figs. 7 and 8 are time series of regionally-averaged HW characteristics. All the HW characteristics exhibit increasing trends regardless of HW definitions. HWF and HWN are generally higher when using T_w to define HWs, while HWA based on T_{max} is higher than that based on $T_{w,\,max}$, and HWA based on T_{min} is lower than that based on $T_{w,\,min}$. In Java, there were around 200 total HW days and 25 HW events during 2016 based on $T_{w,\,min}$. HWF and HWN based on minimum temperatures are higher than those based on maximum temperatures. Though HW characteristics display different magnitudes and change rates in different regions, their time series patterns show very high similarities (correlations are high). The high magnitudes generally coincide with strong El Niño years, i.e., 1983, 1998, 2010 and 2016. This indicates the strong impacts of El Niño on climate extremes in SEA (e.g., Lin et al., 2018). The correlations of HW characteristics with ENSO will be examined in the next section.

Table 1 lists the trends of regionally-averaged HW characteristics based on different thresholds. All the trends are positive and statistically significant, signifying more frequent, longer, and more intense HWs in all the regions in SEA. For all regions, HW characteristics based on minimum temperatures show faster increasing trends than their counterparts based on maximum temperatures, except HWA in Malay Peninsula and Borneo. Among different regions, HW characteristics based on T and T_w also display some dissimilarities. For the IndoChina Peninsula, HWs based on T_w show faster trends than their counterparts based on T; while for Sumatra, Borneo, and Java, the reverse is true. For the Malay Peninsula, the comparison gives mixed results: HW characteristics based on TX90pct increase more slowly than the corresponding characteristics based on TWX90pct, while those based on TN90pct show faster increasing trends than their counterparts based on TWN90pct.

Table 1
Trends of regionally-averaged heatwave characteristics. The units are days/decade for HWF, events/decade for HWN and °C/decade for HWA. All the trends are statistically significant at 95% level.

Regions	Thresholds	HWF	HWN	HWA
Malay Peninsula	TX90pct	3.35 ± 2.64	0.90 ± 0.65	0.45 ± 0.36
	TN90pct	6.70 ± 3.38	1.70 ± 0.80	0.65 ± 0.16
	TWX90pct	4.05 ± 1.73	1.12 ± 0.45	0.66 ± 0.15
	TWN90pct	5.64 ± 2.56	1.44 ± 0.59	0.56 ± 0.10
Sumatra	TX90pct	4.64 ± 1.54	1.03 ± 0.29	0.51 ± 0.17
	TN90pct	7.52 ± 2.79	1.85 ± 0.62	0.58 ± 0.16
	TWX90pct	2.04 ± 1.15	0.58 ± 0.32	0.30 ± 0.12
	TWN90pct	6.14 ± 2.21	1.52 ± 0.52	0.46 ± 0.11
Borneo	TX90pct	5.21 ± 1.93	1.28 ± 0.40	0.79 ± 0.20
	TN90pct	5.18 ± 2.43	1.36 ± 0.63	0.56 ± 0.13
	TWX90pct	3.03 ± 1.36	0.87 ± 0.40	0.50 ± 0.14
	TWN90pct	4.90 ± 2.25	1.29 ± 0.58	0.45 ± 0.11
Java	TX90pct	3.63 ± 2.69	0.92 ± 0.67	0.34 ± 0.23
	TN90pct	5.66 ± 2.02	1.46 ± 0.49	0.63 ± 0.14
	TWX90pct	1.84 ± 1.20	0.48 ± 0.32	0.25 ± 0.20
	TWN90pct	5.38 ± 1.87	1.34 ± 0.43	0.51 ± 0.18
IndoChina	TX90pct	7.78 ± 2.91	1.54 ± 0.52	0.63 ± 0.25
	TN90pct	8.78 ± 2.58	1.96 ± 0.57	0.76 ± 0.18
	TWX90pct	7.56 ± 2.75	1.83 ± 0.63	0.74 ± 0.18
	TWN90pct	11.0 ± 2.95	2.39 ± 0.58	0.84 ± 0.26

3.2. Impact of ENSO and IOD

Figs. 7 and 8 show that the high magnitudes of HWF and HWN generally coincide with strong El Niño years. Across different regions, Java shows strongest responses to El Niño in HWF and HWN, especially when based on T_w, while IndoChina Peninsula shows highest HWA, especially after 1998. To quantify the impact of ENSO on the HW characteristics in various regions, the non-parametric Spearman's correlation coefficients between ONI and detrended HW characteristics are listed in Table 2. With few exceptions, all HW characteristics across different regions show statistically significant correlations with ONI at 95% level. For IndoChina Peninsula and Malay Peninsula, the HW characteristics based on T_w generally show lower correlation coefficients than those based on T. For Java, Borneo, and Sumatra, the correlation coefficients for T- and T_w-based HW characteristics are comparable, indicating that ENSO impacts the HWs based on dry- and wet-bulb temperatures equally in these regions. Some notable exceptions are observed for HWA, which shows statistically insignificant correlations in Sumatra based on TX90pct, and in IndoChina based on T_w. This may be related to the definition of HWA in this study, which is a relative quantity (i.e., the temperature exceedance above the thresholds), while HWN and HWF are defined based on absolute values. Consequently,

Table 2
Spearman's correlation coefficients of the detrended regionally-averaged heatwave characteristics and Oceanic Niño Index (ONI) in DJF (December, January, and February). Shown in parentheses are the corresponding p-values, which are omitted if $p<0.05$.

Regions	Threasholds	HWF	HWN	HWA
Malay Peninsula	TX90pct	0.46	0.48	0.47
	TN90pct	0.49	0.48	0.59
	TWX90pct	0.25(0.11)	0.28(0.08)	0.47
	TWN90pct	0.53	0.52	0.66
Sumatra	TX90pct	0.31(0.05)	0.35	0.26(0.10)
	TN90pct	0.40	0.43	0.56
	TWX90pct	0.62	0.63	0.71
	TWN90pct	0.51	0.52	0.66
Borneo	TX90pct	0.35	0.32	0.36
	TN90pct	0.37	0.38	0.53
	TWX90pct	0.33	0.32	0.41
	TWN90pct	0.42	0.42	0.56
Java	TX90pct	0.52	0.52	0.52
	TN90pct	0.39	0.36	0.44
	TWX90pct	0.44	0.46	0.35
	TWN90pct	0.39	0.41	0.40
IndoChina	TX90pct	0.49	0.55	0.60
	TN90pct	0.53	0.57	0.46
	TWX90pct	0.25(0.13)	0.27(0.09)	0.13(0.41)
	TWN90pct	0.33	0.36	0.10(0.55)

Table 3
Spearman's correlation coefficients of the detrended regionally-averaged heatwave characteristics and Dipole Mode Index (DMI). Shown in parentheses are the corresponding *p*-values, which are omitted if $p<0.05$.

Regions	Thresholds	HWF	HWN	HWA
Malay Peninsula	TX90pct	−0.15(0.37)	−0.14(0.40)	−0.09(0.60)
	TN90pct	−0.24(0.13)	−0.23(0.16)	−0.27(0.10)
	TWX90pct	−0.09(0.57)	−0.11(0.50)	−0.14(0.38)
	TWN90pct	−0.23(0.15)	−0.22(0.17)	−0.33
Sumatra	TX90pct	0.10(0.56)	0.07(0.65)	0.16(0.33)
	TN90pct	−0.06(0.69)	−0.05(0.76)	0.07(0.67)
	TWX90pct	−0.27(0.09)	−0.29(0.07)	−0.32
	TWN90pct	−0.15(0.34)	−0.16(0.31)	−0.16(0.33)
Borneo	TX90pct	0.07(0.65)	0.08(0.61)	0.06(0.72)
	TN90pct	−0.10(0.55)	−0.10(0.55)	−0.06(0.72)
	TWX90pct	−0.11(0.49)	−0.11(0.52)	−0.24(0.14)
	TWN90pct	−0.13(0.42)	−0.13(0.41)	−0.14(0.40)
Java	TX90pct	−0.04(0.82)	−0.06(0.71)	0.11(0.49)
	TN90pct	−0.23(0.15)	−0.25(0.13)	−0.41
	TWX90pct	−0.58	−0.58	−0.71
	TWN90pct	−0.39	−0.40	−0.66
IndoChina	TX90pct	−0.09(0.58)	−0.16(0.33)	−0.17(0.31)
	TN90pct	−0.10(0.56)	−0.12(0.44)	−0.10(0.54)
	TWX90pct	0.02(0.92)	−0.00(0.99)	0.07(0.68)
	TWN90pct	−0.06(0.71)	−0.08(0.63)	0.01(0.98)

the correlations between HWA and ONI are more geographically dependent than those for the other two characteristics.

Table 3 lists the Spearman's correlation coefficients between DMI and detrended HW characteristics. DMI and HW characteristics are generally negatively correlated, since negative IOD causes warming in the Sumatra coast. The only region that shows statistically significant correlation coefficients is Java for HW characteristics based on T_w. In IndoChina Peninsula, the coefficients are very close to zero with high *p*-values, indicating that the impacts of IOD are quite small, if not negligible. In other regions, the coefficients are between −0.3 and −0.1, showing limited influence of IOD. It should be noted that we only quantify the effects of ENSO and IOD on HW characteristics, without considering the interactions between ENSO and IOD, and the possible impacts associated with these interactions.

3.3. Comparison with other reanalysis datasets

Here we further test the robustness of the above findings based on ERA5. Generally, trends of HW characteristics from different reanalysis datasets are consistent, especially the trends based on the minimum temperatures are larger than those based on the maximum temperatures. For brevity, Table. 4 only shows HWF based on T_{min} and $T_{w,\ min}$ from different reanalysis datasets. These HWF from different reanalysis datasets show quite consistent and statistically significant increasing trends, although the specific numbers vary. In the IndoChina Peninsula, the trends based on $T_{w,\ min}$ are higher than those based on T_{min}, except in CFSR. In other regions, the comparison between trends based on T_{min} and $T_{w,\ min}$ is complicated, and not always consistent with that based on ERA5. This demonstrates that there are still many inconsistencies across different reanalysis datasets, as shown by Schoof et al. (2017) in evaluating different reanalysis datasets for HWs in US.

Table 4
Comparison of trends of regionally-averaged HWF(TN90pct) and HWF(TWN90pct) from different reanalysis datasets. All are statistically significant at 95% level. The units are days/decade. MP: Malay Peninsula; SM: Sumatra; BN: Borneo; JA: Java; and IC: IndoChina Peninsula.

HWF(TN90pct)	MP	SM	BN	JA	IC
ERA5	6.70	7.52	5.18	5.66	8.78
ERA-Interim	2.33	5.03	5.32	4.4	6.09
MERRA2	7.07	5.47	4.19	4.32	6.21
CFSR	8.27	7.54	5.65	6.63	9.16
HWF(TWN90pct)	MP	SM	BN	JA	IC
ERA5	5.64	6.14	4.90	5.38	11.0
ERA-Interim	6.55	4.46	7.15	7.18	9.86
MERRA2	7.23	5.83	5.12	4.55	9.41
CFSR	9.12	6.84	5.68	6.82	8.75

4. Discussions and conclusions

The present study analysed the heat wave (HW) characteristics (frequency, duration and intensity) from 1979 to 2018 in Southeast Asia, a region largely unexplored previously but climatologically important. Due to the data scarceness in this region, a new, state-of-the-art reanalysis dataset, ERA5, from ECMWF was utilized to calculate those HW characteristics based on both (dry-bulb) air temperature and wet-bulb temperature. Our study showed that all characteristics (HWF, HWN and HWA) based on various HW definitions exhibit increasing trends in SEA, although their magnitudes and statistical significance vary across different regions. This is consistent with the more frequent, longer-lasting and more intense HW characteristics globally. Of particular interest is that HWs based on wet-bulb temperatures show mostly larger trends than those based on dry-bulb temperatures in the Malay Peninsula and IndoChina Peninsula, indicating the important part played by humidity. Also of great health concern is that HWs based on minimum temperatures are increasing at a much higher rate than their counterparts based on maximum temperature, since high nighttime temperatures can lead to higher mortality rate during HWs (Ho et al., 2017).

To our limited knowledge, the present study is the first comprehensively looking into HW characteristics in SEA. Luo and Lau (2018) investigated the HW trends in the IndoChina Peninsula based on dry-bulb temperature using CFSR from 1979 to 2010. Although they used different definition of HW from ours, surprisingly our results agree well with their trends of HWF (3.75 and 14.0 days/decade for dry and wet seasons, respectively) and HWA (0.34 and 1.05 °C/decade for dry and wet seasons, respectively). Their trends of HWN are rather small (0.45 and 0.87 events/decade for dry and wet seasons, respectively), since they calculated the trends for dry and wet seasons separately. This good agreement demonstrates that our analyses of HW characteristics are robust and that humidity is responsible for the large increasing trends seen in our study. Further tests with several other reanalysis datasets also showed that our findings are generally robust, although some inconsistencies existed across different datasets.

While studies of climate extremes based on reanalysis data are emerging in regions with scarce or unreliable observations, cautions should be taken and careful validation against high-quality observation data (when they become available) is strongly desirable (Grotjahn et al., 2016). Further investigations will focus on the relation between HW and climate variability, large scale atmospheric circulation and land-atmosphere interactions. For example, ENSO and IOD are known to impact the temperature and precipitation in SEA, as demonstrated in the present study and Thirumalai et al. (2017). The present study has shown that ENSO and IOD impact HWs in different regions in different ways; yet the mechanisms of ENSO and IOD's contributions to HWs are to be further studied and quantified. Future changes of HWs under different climate change scenarios are also of great concern to the SEA's policy makers and general public.

CRediT authorship contribution statement

Xian-Xiang Li: Conceptualization, Methodology, Data curation, Writing - original draft, Visualization, Investigation, Writing - review & editing.

Acknowledgments

This research was supported by the National Research Foundation Singapore (NRF) under its Campus for Research Excellence and Technological Enterprise (CREATE) programme, and Sun Yat-sen University's 'One-Hundred Talents' programme. The European Center for Medium-Range Weather Forecasting (ECMWF) is acknowledged for providing ERA5 reanalysis data. These data can be downloaded from the Copernicus Climate Change Service (C3S) Climate Date Store (https://cds.climate.copernicus.eu/cdsapp#!/dataset/reanalysis-era5-single-levels?tab=form). We acknowledge the SA-OBS dataset and the data providers in the SACA&D project (http://saca-bmkg.knmi.nl). The script for calculating the wet-bulb temperature can be downloaded from https://github.com/smartlixx/WetBulb.

Declaration of competing interest

The authors declare that they have no known competing financial interests or personal relationships that could have appeared to influence the work reported in this paper.

References

Albergel, C., Dutra, E., Munier, S., Calvet, J.-C., Munoz-Sabater, J., de Rosnay, P., Balsamo, G., 2018. ERA-5 and ERA-Interim driven ISBA land surface model simulations: which one performs better? Hydrol. Earth Syst. Sci. 22 (6), 3515. https://doi.org/10.5194/hess-22-3515-2018.

Alexander, L., Zhang, X., Peterson, T., Caesar, J., Gleason, B., Klein Tank, A., Haylock, M., Collins, D., Trewin, B., Rahimzadeh, F., et al., 2006. Global observed changes in daily climate extremes of temperature and precipitation. J. Geophys. Res.: Atmos. (D5), 1110 https://doi.org/10.1029/2005JD006290.

Betts, A.K., Chan, D.Z., Desjardins, R.L., 2019. Near-surface biases in ERA5 over the Canadian prairies. Frontiers in Environmental Science 7, 129. https://doi.org/10.3389/fenvs.2019.00129.

Caesar, J., Alexander, L.V., Trewin, B., Tse-Ring, K., Sorany, L., Vuniyayawa, V., Keosavang, N., Shimana, A., Htay, M.M., Karmacharya, J., et al., 2011. Changes in temperature and precipitation extremes over the Indo-Pacific region from 1971 to 2005. Int. J. Climatol. 31 (6), 791–801. https://doi.org/10.1002/joc.2118.

Chen, X., Pauluis, O.M., Leung, L.R., Zhang, F., 2020. Significant contribution of mesoscale overturning to tropical mass and energy transport revealed by the ERA5 reanalysis. Geophys. Res. Lett. https://doi.org/10.1029/2019GL085333.

Cheong, W.K., Timbal, B., Golding, N., Sirabaha, S., Kwan, K.F., Cinco, T.A., Archevarahuprok, B., Vo, V.H., Gunawan, D., Han, S., 2018. Observed and modelled temperature and precipitation extremes over Southeast Asia from 1972 to 2010. Int. J. Climatol. 38 (7), 3013–3027. https://doi.org/10.1002/joc.5479.

Coates, L., Haynes, K., O'Brien, J., McAneney, J., De Oliveira, F.D., 2014. Exploring 167 years of vulnerability: an examination of extreme heat events in Australia 1844–2010. Environ. Sci. Pol. 42, 33–44. https://doi.org/10.1016/j.envsci.2014.05.003.

Coffel, E.D., Horton, R.M., de Sherbinin, A., 2017. Temperature and humidity based projections of a rapid rise in global heat stress exposure during the 21st century. Environ. Res. Lett. 13 (1), 14001. https://doi.org/10.1088/1748-9326/aaa00e.

Copernicus Climate Change Service. ERA5: Fifth Generation of ECMWF Atmospheric Reanalyses of the Global Climate, 2017. URL https://cds.climate.copernicus.eu/cdsapp#!/home. Accessed on 2019-01-30.

D'Arrigo, R., Wilson, R., 2008. El Nino and Indian Ocean influences on Indonesian drought: implications for forecasting rainfall and crop productivity. Int. J. Climatol. 28 (5), 611–616. https://doi.org/10.1002/joc.1654.

Davies-Jones, R., 2008. An efficient and accurate method for computing the wet-bulb temperature along pseudoadiabats. Mon. Weather Rev. 136 (7), 2764–2785. https://doi.org/10.1175/2007MWR2224.1.

Davis, R.E., McGregor, G.R., Enfield, K.B., 2016. Humidity: a review and primer on atmospheric moisture and human health. Environ. Res. 144, 106–116. https://doi.org/10.1016/j.envres.2015.10.014.

Dee, D.P., Uppala, S.M., Simmons, A.J., Berrisford, P., Poli, P., Kobayashi, S., Andrae, U., Balmaseda, M.A., Balsamo, G., Bauer, D.P., et al., 2011. The ERA-Interim reanalysis: configuration and performance of the data assimilation system. Q. J. R. Meteorol. Soc. 137 (656), 553–597. https://doi.org/10.1002/qj.828.

Dunne, J.P., Stouffer, R.J., John, J.G., 2013. Reductions in labour capacity from heat stress under climate warming. Nat. Clim. Chang. 30 (6), 563. https://doi.org/10.1038/nclimate1827.

Epstein, Y., Moran, D.S., 2006. Thermal comfort and the heat stress indices. Ind. Health 44 (3), 388–398. https://doi.org/10.2486/indhealth.44.388.

Fischer, E.M., Schär, C., 2010. Consistent geographical patterns of changes in high-impact European heatwaves. Nat. Geosci. 30 (6), 398. https://doi.org/10.1038/ngeo866.

Gelaro, R., McCarty, W., Suárez, M.J., Todling, R., Molod, A., Takacs, L., Randles, C.A., Darmenov, A., Bosilovich, M.G., Reichle, R., Wargan, K., 2017. The modern-era retrospective analysis for research and applications, version 2 (MERRA-2). J. Clim. 30 (14), 5419–5454. https://doi.org/10.1175/JCLI-D-16-0758.1.

Gosling, S.N., Lowe, J.A., McGregor, G.R., Pelling, M., Malamud, B.D., 2009. Associations between elevated atmospheric temperature and human mortality: a critical review of the literature. Clim. Chang. 92 (3–4), 299–341. https://doi.org/10.1007/s10584-008-9441-x.

Graham, R.M., Hudson, S.R., Maturilli, M., 2019. Improved performance of ERA5 in Arctic gateway relative to four global atmospheric reanalyses. Geophys. Res. Lett. 46 (11), 6138–6147. https://doi.org/10.1029/2019GL082781.

Grotjahn, R., Black, R., Leung, R., Wehner, M.F., Barlow, M., Bosilovich, M., Gershunov, A., Gutowski, W.J., Gyakum, J.R., Katz, R.W., et al., 2016. North American extreme temperature events and related large scale meteorological patterns: a review of statistical methods, dynamics, modeling, and trends. Clim. Dyn. 46 (3–4), 1151–1184. https://doi.org/10.1007/s00382-015-2638-6.

Hassim, M.E., Timbal, B., 2019. Observed rainfall trends over Singapore and the Maritime Continent from the perspective of regional-scale weather regimes. J. Appl. Meteorol. Climatol. 58 (2), 365–384.

Hennermann, K., Berrisford, P., 2018. What are the changes from ERA-Interim to ERA5?. URL https://confluence.ecmwf.int/pages/viewpage.action?pageId=74764925

Ho, H.C., Lau, K.K.-L., Ren, C., Ng, E., 2017. Characterizing prolonged heat effects on mortality in a sub-tropical high-density city, Hong Kong. Int. J. Biometeorol. 61 (11), 1935–1944. https://doi.org/10.1007/s00484-017-1383-4 0.

Hoffmann, L., Günther, G., Li, D., Stein, O., Wu, X., Griessbach, S., Heng, Y., Konopka, P., Müller, R., Vogel, B., et al., 2019. From ERA-Interim to ERA5: the considerable impact of ECMWF's next-generation reanalysis on Lagrangian transport simulations. Atmos. Chem. Phys. 19 (5), 3097–3124. https://doi.org/10.5194/acp-19-3097-2019 0.

Hong, C.-C., Li, T., 2009. The extreme cold anomaly over Southeast Asia in February 2008: roles of ISO and ENSO. J. Clim. 22 (13), 3786–3801. https://doi.org/10.1175/2009JCLI2864.1 0.

Huang, C., Cheng, J., Phung, D., Tawatsupa, B., Hu, W., Xu, Z., 2018. Mortality burden attributable to heatwaves in Thailand: a systematic assessment incorporating evidence-based lag structure. Environ. Int. 121 (0), 41–50. https://doi.org/10.1016/j.envint.2018.08.058.

Im, E.-S., Kang, S., Eltahir, E.A.B., 2018. Projections of rising heat stress over the western Maritime Continent from dynamically downscaled climate simulations. Glob. Planet. Chang. 165 (0), 160–172. https://doi.org/10.1016/j.gloplacha.2018.02.014.

IPCC, 2007. Climate Change 2007: The Physical Science Basis. Working Group I Contribution to the Fourth Assessment Report of the Intergovernmental Panel on Climate Change. Cambridge University Press, New York.

Li, J., Chen, Y.D., Gan, T.Y., Lau, N.-C., 2018. Elevated increases in human-perceived temperature under climate warming. Nat. Clim. Chang. 80 (1), 43. https://doi.org/10.1038/s41558-017-0036-2 0.

Li, X.-X., 2018. Linking residential electricity consumption and outdoor climate in a tropical city. Energy 157, 734–743. https://doi.org/10.1016/j.energy.2018.05.192 0.

Lin, L., Chen, C., Luo, M., 2018. Impacts of El Niño–Southern Oscillation on heat waves in the Indochina peninsula. Atmos. Sci. Lett. 19 (11), e856. https://doi.org/10.1002/asl.856 0.

Luo, M., Lau, N.-C., 2018. Synoptic characteristics, atmospheric controls, and long-term changes of heat waves over the Indochina peninsula. Clim. Dyn. 51 (0), 2707–2723. https://doi.org/10.1007/s00382-017-4038-6.

Mahto, S.S., Mishra, V., 2019. Does ERA-5 outperform other reanalysis products for hydrologic applications in India? J. Geophys. Res.: Atmos. 124 (16), 9423–9441. https://doi.org/10.1029/2019JD031155 0.

Mann, H.B., 1945. Nonparametric tests against trend. Econometrica 130 (3), 245–259 0.

Manton, M.J., Della-Marta, P.M., Haylock, M.R., Hennessy, K.J., Nicholls, N., Chambers, L.E., Collins, D.A., Daw, G., Finet, A., Gunawan, D., et al., 2001. Trends in extreme daily rainfall and temperature in Southeast Asia and the South Pacific: 1961–1998. Int. J. Climatol. 21 (3), 269–284. https://doi.org/10.1002/joc.610 0.

Mora, C., Dousset, B., Caldwell, I.R., Powell, F.E., Geronimo, R.C., Bielecki, C.R., Counsell, C.W., Dietrich, B.S., Johnston, E.T., Louis, L.V., et al., 2017. Global risk of deadly heat. Nat. Clim. Chang. 70 (7), 501. https://doi.org/10.1038/nclimate3322 0.

Nissan, H., Burkart, K., Coughlan de Perez, E., Van Aalst, M., Mason, S., 2017. Defining and predicting heat waves in Bangladesh. J. Appl. Meteorol. Climatol. 56 (10), 2653–2670. https://doi.org/10.1175/JAMC-D-17-0035.1 0.

NWS, 2018. 79-year list of severe weather fatalities. URL. https://www.nws.noaa.gov/om/hazstats/resources/79years.pdf.

Perkins, S.E., Alexander, L.V., 2013. On the measurement of heat waves. J. Clim. 26 (13), 4500–4517. https://doi.org/10.1175/JCLI-D-12-00383.1 0.

Perkins, S.E., Alexander, L.V., Nairn, J.R., 2012. Increasing frequency, intensity and duration of observed global heatwaves and warm spells. Geophys. Res. Lett. 39 (20), L20714. https://doi.org/10.1029/2012GL053361 0.

Perkins-Kirkpatrick, S.E., Gibson, P.B., 2017. Changes in regional heatwave characteristics as a function of increasing global temperature. Sci. Rep. 70 (1), 12256. https://doi.org/10.1038/s41598-018-23085-z 0.

Pielke Sr., R.A., Davey, C., Morgan, J., 2004. Assessing "global warming" with surface heat content. Eos, Transactions of American Geophysical Union 85 (21), 210–211. https://doi.org/10.1029/2004EO210004.

Raymond, C., Singh, D., Horton, R., 2017. Spatiotemporal patterns and synoptics of extreme wet-bulb temperature in the contiguous United States. J. Geophys. Res.: Atmos. (24), 1220 https://doi.org/10.1002/2017JD027140.

Russo, S., Sillmann, J., Sterl, A., 2017. Humid heat waves at different warming levels. Sci. Rep. 70 (1), 7477. https://doi.org/10.1038/s41598-017-07536-7 0.

Saha, S., Moorthi, S., Pan, H.-L., Wu, X., Wang, J., Nadiga, S., Tripp, P., Kistler, R., Woollen, J., Behringer, D., Liu, H., Stokes, D., Grumbine, R., Gayno, G., Wang, J., Hou, Y.-T., Chuang, H.-Y., Juang, H.-M.H., Sela, J., Iredell, M., Treadon, R., Kleist, D., Delst, P.V., Keyser, D., Derber, J., Ek, M., Meng, J., Wei, H., Yang, R., Lord, S., van den Dool, H., Kumar, A., Wang, W., Long, C., Chelliah, M., Xue, Y., Huang, B., Schemm, J.-K., Ebisuzaki, W., Lin, R., Xie, P., Chen, M., Zhou, S., Higgins, W., Zou, C.-Z., Liu, Q., Chen, Y., Han, Y.,

Cucurull, L., Reynolds, R.W., Rutledge, G., Goldberg, M., 2010. NCEP Climate Forecast System Reanalysis (CFSR) Selected Hourly Time-Series Products, January 1979 to December 2010.
Saji, N.H., Goswami, B.N., Vinayachandran, P.N., Yamagata, T., 1999. A dipole mode in the tropical Indian Ocean. Nature 401 (0), 360–363.
Schär, C., 2016. The worst heat waves to come. Nat. Clim. Chang. 60 (2), 128. https://doi.org/10.1038/nclimate2864 0.
Schoof, J.T., Ford, T.W., Pryor, S.C., 2017. Recent changes in U.S. regional heat wave characteristics in observations and reanalyses. J. Appl. Meteorol. Climatol. 56 (9), 2621–2636. https://doi.org/10.1175/JAMC-D-16-0393.1 0.
Sen, P.K., 1968. Estimates of the regression coefficient based on Kendall's tau. J. Am. Stat. Assoc. 63 (324), 1379–1389 0.
Sherwood, S.C., 2018. How important is humidity in heat stress? J. Geophys. Res.: Atmos. 123 (21), 11808–11810. https://doi.org/10.1029/2018JD028969.
Sherwood, S.C., Huber, M., 2010. An adaptability limit to climate change due to heat stress. Proc. Natl. Acad. Sci. 107 (21), 9552–9555. https://doi.org/10.1073/pnas.0913352107.
Tangang, F., Farzanmanesh, R., Mirzaei, A., Salimun, E., Jamaluddin, A.F., Juneng, L., 2017. Characteristics of precipitation extremes in Malaysia associated with El Niño and La Niña events. Int. J. Climatol. 37 (0), 696–716. https://doi.org/10.1002/joc.5032.
Tangang, F.T., Juneng, L., Salimun, E., Vinayachandran, P.N., Seng, Y.K., Reason, C.J., Behera, S.K., Yasunari, T., 2008. On the roles of the northeast cold surge, the Borneo vortex, the Madden-Julian Oscillation, and the Indian Ocean Dipole during the extreme 2006/2007 flood in southern Peninsular Malaysia. Geophys. Res. Lett. 35 (14), L14S07. https://doi.org/10.1029/2008GL033429.
Tarek, M., Brissette, F.P., Arsenault, R., 2019. Evaluation of the ERA5 reanalysis as a potential reference dataset for hydrological modeling over North-America. Hydrol. Earth Syst. Sci. Discuss. 2019 (0), 1–35. https://doi.org/10.5194/hess-2019-316.
Thirumalai, K., DiNezio, P.N., Okumura, Y., Deser, C., 2017. Extreme temperatures in Southeast Asia caused by El Niño and worsened by global warming. Nat. Commun. 8, 15531. https://doi.org/10.1038/ncomms15531.
Van den Besselaar, E.J., Van der Schrier, G., Cornes, R.C., Iqbal, A.S., Klein Tank, A.M., 2017. SA-OBS: a daily gridded surface temperature and precipitation dataset for Southeast Asia. J. Clim. 30 (14), 5151–5165. https://doi.org/10.1175/JCLI-D-16-0575.1 0.
Villafuerte, M.Q., Matsumoto, J., 2015. Significant influences of global mean temperature and ENSO on extreme rainfall in Southeast Asia. J. Clim. 28 (5), 1905–1919. https://doi.org/10.1175/JCLI-D-14-00531.1.
Wehner, M., Stone, D., Krishnan, H., AchutaRao, K., Castillo, F., 2016. The deadly combination of heat and humidity in India and Pakistan in summer 2015. Bull. Am. Meteorol. Soc. 97 (12), S81–S86. https://doi.org/10.1175/BAMS-D-16-0145.1.
Willett, K.M., Sherwood, S., 2012. Exceedance of heat index thresholds for 15 regions under a warming climate using the wet-bulb globe temperature. Int. J. Climatol. 32 (2), 161–177. https://doi.org/10.1002/joc.2257 0.
Xia, Y., Li, Y., Guan, D., Tinoco, D.M., Xia, J., Yan, Z., Yang, J., Liu, Q., Huo, H., 2018. Assessment of the economic impacts of heat waves: a case study of Nanjing, China. J. Clean. Prod. 171, 811–819. https://doi.org/10.1016/j.jclepro.2017.10.069 0.
Xu, Z., FitzGerald, G., Guo, Y., Jalaludin, B., Tong, S., 2016. Impact of heatwave on mortality under different heatwave definitions: a systematic review and meta-analysis. Environ. Int. 89 (0), 193–203. https://doi.org/10.1016/j.envint.2016.02.007.